

Finite element analysis of pre and post penetration behavior of surface cracks in pipes

T.Miyoshi

Faculty of Engineering, University of Tokyo, Japan

M.Shiratori

Faculty of Engineering, Yokohama National University, Japan

1 INTRODUCTION

In the present paper the authors have carried out a series of elastic-plastic analyses for the circumferentially cracked pipes loaded in four-point bending. They have obtained the load-displacement, the J-displacement curves and the crack opening area for the cracks with various configurations. Based upon these curves an engineering approach has been applied to estimate the stable growth and instability of a surface crack. The Battelle's experiment about the crack growth has been estimated well by this analysis. Finally the results have been compared with those obtained by the line spring method.

2 FINITE ELEMENT ANALYSIS FOR STATIONARY CRACKS

2.1 Method of Analysis

The authors have developed a three dimensional finite element code, FEM3D, in order to analyze the elastic-plastic problems of three dimensional surface cracks by a supercomputer (Miyoshi 1986a). In the elastic-plastic analysis the J_2 flow theory is assumed and the incremental method originally proposed by Marcal (Marcal 1967) is adopted. The number of iterations in each incremental stage is two. The J-integral is evaluated by the virtual crack extension (VCE) method (Parks 1978).

In this paper three dimensional elastic-plastic analyses have been carried out for the Battelle round-robin problem (Ahmad 1986). The analyses have been done for eight different crack configurations, that is, four part-through cracks (Fig. 1(a)) and four through cracks (Fig. 1(b)). These crack configurations have been chosen to supply the data for the estimation of crack growth in the next section. For the part-through cracks in Fig. 1(a) the depths of the cracks are chosen to be

$$a/t = 0.662, 0.7, 0.8 \text{ and } 0.9$$

where a is the depth of the crack at $\theta = 0^\circ$ and t is the thickness of the pipe. The crack of $a/t = 0.662$ is the case of the Battelle round-robin. In this case the depth of the crack is uniform along the circumferential direction. In the other three cases the configurations of

θ	0°	15°	30°	45°	60°	75°	95.76°
Δd	Δa	$\frac{5}{6}\Delta a$	$\frac{4}{6}\Delta a$	$\frac{3}{6}\Delta a$	$\frac{2}{6}\Delta a$	$\frac{1}{6}\Delta a$	0

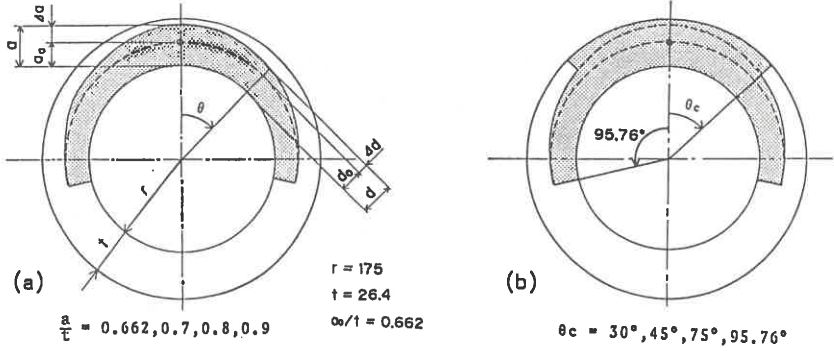


Fig.1 Geometry of (a) part-through and (b) through cracks.

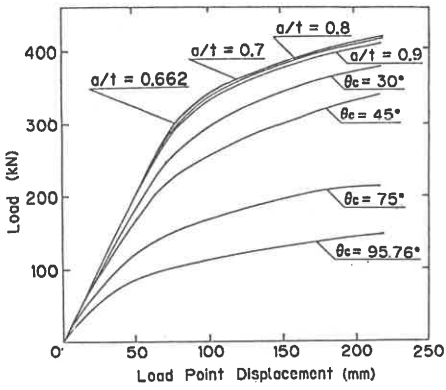


Fig.2 Load versus load-point-displacement curves.

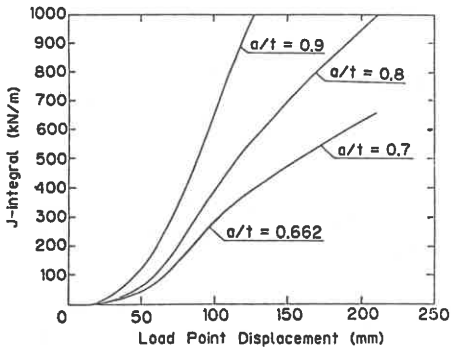


Fig.3 J versus load-point-displacement curves for the part-through cracks.

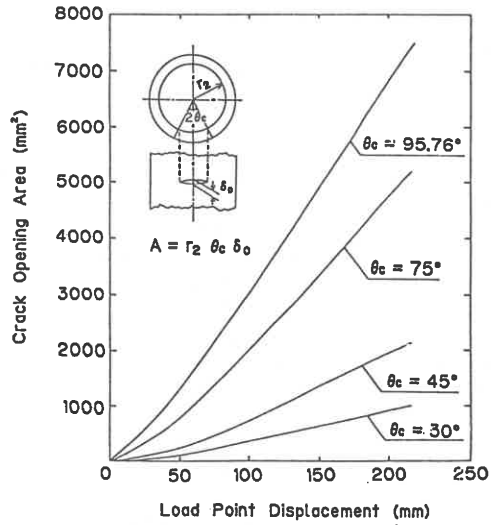


Fig.4 Crack opening area versus load-point-displacement curves for the through cracks.

the cracks are determined in such a way as shown in the table attached to Fig. 1(a) where d is the depth of the crack at θ and $\Delta d = d - a_0$ with $a_0 = 0.662t$. The configuration of the through crack is shown in Fig. 1(b). It is assumed that the part of $|\theta| < \theta_c$ has penetrated through the thickness from the part-through crack of $a/t = 0.9$.

Twenty noded (brick type) and fifteen noded (triangular prism) isoparametric elements with quadratic shape functions are used and Barsoum's singular elements (Barsoum 1977) are utilized at the crack tip. The numbers of elements and nodes are 165 and 1073, respectively. The experimentally obtained uniaxial true stress versus true strain curve has been approximated by piecewise linear curves in the FEM calculations.

2.2 Results

Fig. 2 shows the load versus displacement curves for every cases calculated. The curves of $a/t = 0.662, 0.7, 0.8$ and 0.9 are the results for the part-through cracks while those of $\theta_c = 30^\circ, 45^\circ, 75^\circ$ and 95.76° are the results for the through cracks. These curves show that the load-carrying-capacity falls down rapidly when a crack penetrate through the thickness. Fig. 3 shows the J versus displacement curves for every case of the part-through crack. Fig. 4 shows the crack opening area versus displacement curves for every case of the through crack. The crack opening area, A , is approximated by $A = r_2 \theta_c \delta_0$ where δ_0 is the crack opening displacement at $\theta = 0^\circ$. Fig. 4 gives an important information for the detection of leakage, i.e., the flow rate of the coolant through the crack.

3 ANALYSIS OF CRACK GROWTH

3.1 Method of Analysis

An engineering approach has been adopted to estimate the behavior of the crack growth. It is illustrated schematically in Fig. 5. Fig. 5(a) and (b) show $P-\delta$ and $J-\delta$ curves, respectively, for three different stationary cracks whose depths are specified by a_1, a_2 and a_3 , where it is assumed that $a_1 < a_2 < a_3$. In these figures P denotes the load and δ the loadpoint displacement. The estimation scheme of the crack growth followed by the engineering approach is as follows:

Generation Phase: If an experimental $P-\delta$ curve which accompanies the crack growth can be available, one can estimate the $J-R$ curve. If the dotted line ACE in Fig. 5(a) is assumed to be the experimental $P-\delta$ curve, the path of the estimation scheme is expressed by $A \rightarrow B \rightarrow C \rightarrow D \rightarrow E$ in the figure. When the crack of the depth a_1 satisfies the fracture criterion, $J = J_{mat}$, at $\delta = \delta_1$, the crack grows by a certain amount. And then the depth of the crack becomes a_2 . The fracture criterion based upon the $J-R$ curve has been assumed in the analysis. The value of J on the $J-R$ curve is defined by J_{mat} . The process of the above crack growth is assumed to occur with δ held constant. If

it is not the case, the point B falls on somewhere in-between the path BC. There is no problem to postulate the above assumption. If the crack is stable at the point B, it is possible to increase the applied load up to the point C where the fracture criterion is satisfied again, and so forth. If we have an experimental P- δ curve ACE, it is easy to draw the path ABCDE in Fig. 5(a), (b) and (c). And then, one can estimate the J-R curve by plotting the points A, C, E on the J - Δa plane.

Application Phase: The estimation scheme of the application phase is the reversion of the generation phase. If the J-R curve is known previously, one can estimate the P- δ curve with crack growth. The crack of the depth a_1 will grow when $J=J_{mat}$, i.e., at the point A in Fig. 5 (a) and (b). At this point δ is known to be δ_1 , and then one can estimate the corresponding value of P on Fig. 5(a), and so on. Finally one can estimate the P- δ curve corresponding to the J-R curve.

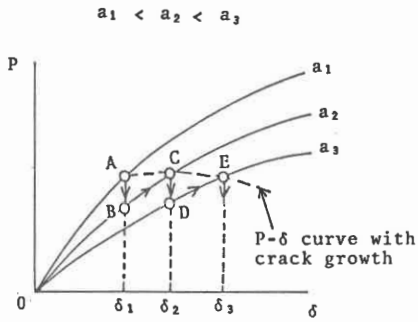
3.2 Results

Generation Phase: In Fig. 6 the load-displacement curves for the part-through cracks are replotted in a different scale. These are the parts of the curves in Fig. 2. In the figure the Battelle's experimental P- δ curve is plotted at the same time. It coincides with the P- δ curve of $a/t=0.662$ before the point A at which the crack initiates to grow. The curve after the crack initiation is expressed by the path of ACE. The notations A, C, and E corresponds to those in Fig. 5. The raw data of the crack growth summarized in the table 1 are from the Battelle round-robin (Ahmad 1986). Since the load point displacements for certain amounts of the crack growth are known from this table, the corresponding values of J can be estimated by the J- δ curves of Fig. 3. The values of J that do not correspond to $a/t = 0.662, 0.7, 0.8$ or 0.9 have been determined by the quadratic interpolation. The open circles in Fig. 7 are the relations of J and Δa which give a J-R curve. The linear curve in the figure is the J-R curve drawn by the least square method. It is expressed by

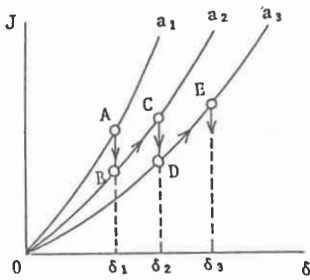
$$(1) \quad J = 68.2\Delta a + 261.9$$

Application Phase: The J-R curve of eq. (1) is assumed. By following the estimation scheme of the application phase described in the previous section, the P- δ curve of ACE in Fig. 6 has been obtained. This means we can estimate the curve which accompanies the crack growth if we know the J-R curve beforehand.

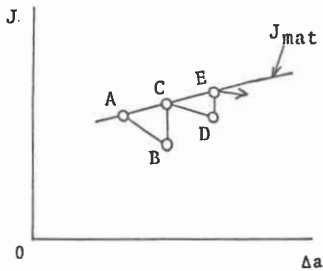
Estimation of Instability: The available experimental data for crack growth were up to $a/t = 0.8$. Therefore, it is difficult to discuss what will happen when the crack grows to $a/t = 0.9$. In Fig. 7 the open square shows the value of J which corresponds to $a/t = 0.9$. This value has been determined as the value of J for δ_E on the J- δ curve of $a/t = 0.9$ in Fig. 3, where δ_E is the value of δ corresponding to the point E in Fig. 6. The above result show that the crack growth from the point E with constant δ would result in the increase of J beyond the J-R curve. Therefore, it



(a)



(b)



(c)

Fig.5 Schematic diagrams that illustrate the engineering approach for the analysis of crack growth.

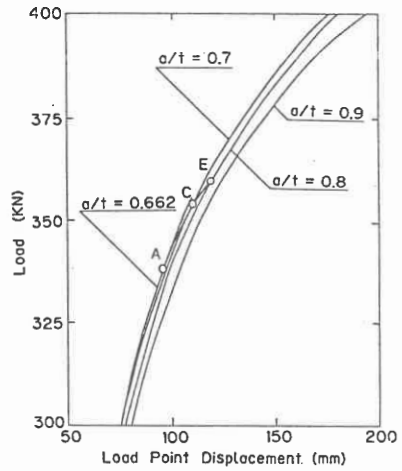


Fig.6 Load versus load-point-displacement curves used in the analysis of crack growth.

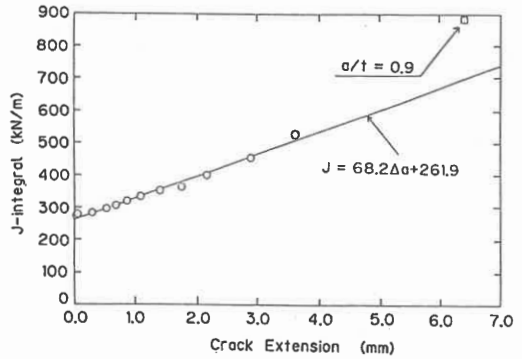


Fig.7 The J-R curve.

Table 1 Load, displacement and crack extension records for the pipe experiment (Ahmad 1986).

Total Load (kN)	Load-Line Displacement (mm)	Crack Extension (mm)
335.2	95.2	0.000
337.8	96.9	.025
341.0	99.4	.050
344.5	101.3	.279
347.3	103.8	.518
349.8	105.8	.686
351.7	108.2	.864
354.1	110.2	1.092
355.8	112.5	1.405
358.7	114.5	1.753
359.9	116.9	2.154
359.9	118.8	2.896
363.8	121.1	3.617

is estimated that the unstable crack growth would have occurred somewhere in-between $a/t = 0.8$ and 0.9 , followed by the immediate penetration.

4 DISCUSSIONS

The authors (Miyoshi 1986b,c) have developed a line spring method by which the J-integral and growth of the surface crack can be analyzed. Some useful informations about the penetration behavior of the surface crack have been obtained through the analysis by the line spring method. The main result of the analysis about the surface cracked line pipe is that instability occurs before penetration in the case of long and shallow crack while that it occurs after penetration in the case of short and deep crack (Miyoshi 1986d). The problem analyzed in the present paper can be regarded as the former case. It has also been shown that the line spring method gives nearly the same values of J-integral as the fully three dimensional finite element analysis (Miyoshi 1986e). This means that the results obtained by the line spring method are enough reliable.

As far as we use the main frame, the fully three dimensional finite element analysis is too time consuming. Therefore, the line spring method is a useful tool for the elastic-plastic analysis of surface cracked plates and shells. But the evaluation of the non-linear compliance of the line spring element is very laborious.

The use of the FEM3D, which runs on the supercomputer, is more attractive because the computing time by this code is about one-fortieth of that by the main frame (Miyoshi 1986a) and one-third of that by the line spring method (Miyoshi 1986e). The analysis of the present paper shows how the FEM3D is useful for the elastic-plastic analysis of the three dimensional crack problems.

REFERENCES

- Ahmad, J., et al. 1986. NUREG/CR-4573 BMI-2135.
Barsoum, R. S. 1977. International J. for Numerical Methods in Engineering 11:85-98.
Marcal, P. V. and King, I. P. 1967. International J. of Mechanical Sciences. 9:143-155
Miyoshi, T., et al. 1986a. Finite Element Methods, Modelling, and New Applications, E.M.Patton, et al. ed. 1986 ASME PVP and CED Conference, Chicago, 115-119.
Miyoshi, T., et al. 1986b. J. of Pressure Vessel Technology, Trans. of ASME. 108:305-311.
Miyoshi, T., et al. 1986c. Engineering Fracture Mechanics. 24-1:103-110.
Miyoshi, T., et al. 1986d. Trans. of JSME. 52:472-475.
Miyoshi, T. and Yoshida, Y. 1986e. Trans. of JSME. 86-0448B.
Parks, D. M. 1978. Numerical Methods in Fracture Mechanics. A. R. Luxmoore and D. R. J.Owen, eds. 464-478.